



# Transmission microscopy without lenses for objects of unlimited size

J.M. Rodenburg\*, A.C. Hurst, A.G. Cullis

*Department of Electronic and Electrical Engineering, University of Sheffield, Mappin Street, Sheffield S1 3JD UK*

Received 11 May 2006; received in revised form 26 July 2006; accepted 26 July 2006

## Abstract

We demonstrate experimentally, for the first time, a new form of lensless microscopy. The image we obtain contains the entire wavefunction emanating from the sample. Large scale, quantitative phase information can be measured, unlike in conventional (Zernike) methods. For light optical experiments, we can dispense with expensive high-quality lenses and the very large working distances available would allow remote monitoring of e.g., environmental cells without compromising resolution. In short wavelength microscopy (X-rays and electrons), where lens components are of very limited numerical aperture, the technique has revolutionary implications: objects of any lateral size or shape can be used and, for transmission electron imaging, resolution down to the scale of the wavelength is likely to be limited only by the presence of atomic vibrations.

© 2006 Elsevier B.V. All rights reserved.

PACS: 42.30.-d; 42.30.Kq; 42.30.Rx; 42.30.Va; 42.30.Wb

Keywords: Phase retrieval; Ptychography; Diffractive imaging; Fourier optics

## 1. Introduction

Conventional transmission microscopy employs a lens which, according to Abbe's theory [1], re-interferes the complex-valued wave disturbance in the Fraunhofer diffraction pattern into an image. If the lens is removed and a detector is placed in the far-field, then it is still possible to calculate, via certain iterative methods [2–6], the object structure despite the loss of all phase information, provided the object is of finite size so that the Nyquist sampling condition in the diffraction plane can be satisfied. In practice, the object needs to be entirely isolated or illuminated by a spatially narrow and well-defined parallel beam (of course, this being limited by the uncertainty principle). Although diffraction methods could be important for short-wavelength X-ray or electron microscopy, where lenses are poor and of very limited numerical aperture, the limited size of the object or illumination renders these phase-retrieval methods very difficult to implement experimentally. The detector must have extre-

mely high resolution, high dynamic range and excellent linearity. Convergence of conventional iterative methods is neither fast nor guaranteed: a typical calculation requires 10,000 Fourier transforms. If this is undertaken over a usefully large data set (1000 × 1000 pixels) the computational demands are considerable. Convergence for certain object classes is not certain, especially for complex objects (in the sense of having both imaginary and real components in the optical potential). Pure diffractive iterative methods (involving the use of just one Fraunhofer diffraction pattern taken from an isolated object) therefore often have to resort to making ad hoc assumptions for each object of interest studied (for example that the object is of weak phase [5]).

Here we show that none of these experimental or theoretical constraints need apply. Indeed, we provide the first demonstration of lensless imaging of an object of unlimited lateral size or unconstrained shape. We use a number (unlimited in practice) of diffraction patterns, recorded from the object which is illuminated by a roughly localised, moveable wave field. Conventional iterative methods cannot easily cope with soft (bandwidth-limited) or complex (phase and modulus) illumination functions.

\*Corresponding author. Tel.: +44 114 222 5391; fax: +44 114 222 5143.  
E-mail address: [j.m.rodenburg@sheffield.ac.uk](mailto:j.m.rodenburg@sheffield.ac.uk) (J.M. Rodenburg).

Indeed, the Fraunhofer diffraction pattern is insensitive to Fresnel propagation near the object plane, and so cannot focus on one layer of a thick object unless a defining aperture is present at that plane [3]. By employing several positions of the same illumination function, our new method picks out one focal plane as with a conventional lens: other planes do not form a self-consistent set of diffraction patterns over the curvature of the Ewald sphere. The redundancy in the data ameliorates artefacts, low counting statistics and poor detector performance. It also leads to spectacular convergence properties: each diffraction pattern needs just one Fourier iteration to produce a reasonable image, although several such patterns must be processed simultaneously. Hence a reasonable quality, wide field-of-view image can be obtained in real-time, as in a conventional microscope.

## 2. Conventional iterative methods

Iterative phase retrieval as originally demonstrated computationally by Gerchberg and Saxton [7] relies on applying measured constraints in more than one plane of intensity information. The planes may be related by Fraunhofer or Fresnel propagation [8,9]. If two such functions are measured in intensity, then only a small subset of possible phases assigned in one of the planes would be consistent with the intensity distribution measured in the one or more other planes. Solution proceeds by applying a random phase to the modulus (square root of intensity) of one such measurement, propagating this complex wave to a second plane (via the known propagation function), and then modifying the modulus so calculated by the measured modulus in the second plane. The calculated phase is retained, and the total resultant complex wave value is back-propagated to the first plane, where the phase so calculated is used as a new estimate in a second iteration, and so on and so forth.

An important modification of this principle, developed by Fienup [2], allows solution of finite objects from just a single Fraunhofer diffraction pattern. In this case, the constraint in real space is that at least half of the object pixels are known to be zero (the object is isolated, surrounded by free space, or delineated by a sharp aperture). The consequence is that, if the object is known to be sufficiently small a priori, it is possible to solve for the object using its diffraction pattern intensity alone. This has been known since the work of Hoppe [10] in the late 1960s: only recently have iterative solution methods made his proposition at least partially viable. The technique, in principle, offers the opportunity to overcome many of the conventional limitations of sub-atomic resolution imaging using X-rays or electrons: all that is required is a laboratory-scale detector positioned in the far field. However, all demonstrations to date (for example Refs. [3–6]) have been able solve only for object functions consisting of less than half the total number of detector

pixels: the factor of one half arises from the constraint in real space described above.

## 3. Experimental demonstration of an improved method

The crucial development we report here relies on being able to move the object of interest (or the illumination) to a number (as large as required) of known positions which span the object, whilst ensuring that adjacent illumination spots overlap. The only limitation on the illumination function is that it must be reasonably localised: it could be formed, for example, from the cross-over of a weak or highly-aberrated lens, from the caustic of a focussing mirror, or simply from a nearby aperture, as we show here. Unlike any previous method reported, our technique can handle any form of incident wave, including complex functions with curved wavefronts and/or soft, bandwidth-limited functions. The only constraint we employ is that this function remains constant as it is moved relative to the object.

In all the work presented here we do not use any imaging lenses. In the first experiment, we *do* use a lens to form a diffraction pattern which has sufficient effective camera length to well satisfy the Fraunhofer condition. This lens is not fundamental in that, without a lens, given sufficient camera length (many metres in the present case) the data we record would be identical. It should be noted that achieving Fraunhofer diffraction with X-ray or electron illumination would be much easier because of the shorter wavelengths involved. In the second experiment, we do not use any lenses whatsoever. The reconstruction is not as impressive for reasons which are easy to explain (the Fraunhofer condition is no longer satisfied). These limitations are not fundamental—they arise from geometric constraints which can be in principle can be accounted for. Furthermore, they only apply to the long-wavelength (optical) applications of the technique.

Our object is an ant about 3 mm in length mounted in resin. It is situated about 1 mm downstream of a simple aperture 0.8 mm in diameter which is illuminated by a spread beam of He–Ne laser light ( $\lambda = 632$  nm). The intensity of illumination at the specimen plane is shown in Fig. 1a. The object is moved on a specimen stage in steps of 0.3 mm over a  $10 \times 10$  grid of points giving overlapped illuminated regions. At each position, a Fraunhofer diffraction pattern is recorded by an ‘off-the-shelf’ 10-bit uncooled CCD camera (an industrial grade Sony XCD-X710): a typical example is shown in Fig. 1b. For each pattern, four exposures of different lengths are used to improve dynamic range. It should be emphasised that our detector has visible read-out noise for which no correction is necessary.

We record the shape of our aperture via a conventional image, and then propagate this function into the Fresnel zone until its intensity matches that recorded in Fig. 1a. In this way we estimate the complex amplitude of our illumination field. We then apply an algorithm for

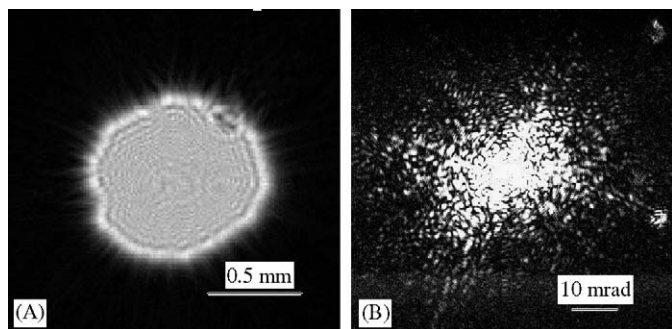


Fig. 1. Experimental data. (A) The illumination function measured in intensity at the object plane. The aperture diameter is 0.8 mm and the object plane is 1 mm downstream of this, hence we see Fresnel interference and broadening of the intensity distribution. A calculated illumination function amplitude, which includes phase changes, and whose intensity matches the above, is used in the reconstruction. Note that conventional methods cannot cope with such complex illumination fields. (B) One of many experimental Fraunhofer diffraction patterns used in the reconstruction. This is the only data we use, but all phase information has been lost. The total angular width of detector is  $4.2^\circ$  (74 mrad): this determines the resolution of the final reconstruction, but is limited in this experiment by geometrical constraints which are not fundamental.

two-dimensional images, the theory of which has been proposed elsewhere [11–13].

One might expect that the three-dimensional structure of our specimen would detrimentally alter the information in the Fraunhofer plane because of phase differences introduced between the top and bottom surfaces of the object: in scattering theory, this is equivalent to the curvature of the Ewald sphere. However, as we show below, direct application of the two-dimensional algorithm gives extraordinarily good results.

The algorithm employs an on-going estimate of the object function which is continually updated. Starting from the neutral assumption that the object space is empty, a calculated exit wave (a product of the complex illumination function and the transmission function of the object) is propagated to the Fraunhofer plane where, as is usual in iterative methods, modulus is replaced by the recorded data and phase preserved. Upon back propagation, the resulting exit wave differs from the previously-calculated exit wave. The difference between these is used to make an update to our current estimate of the object function, weighted according to the modulus and phase of the illuminating function at each point over the object.

Let  $O_{g,n+1}(\mathbf{r})$  be the next guess of our specimen (object) transmission function, where the subscript  $g$  indicates an estimate (guess) of the object function, and subscript  $n$  refers to the  $n$ th iteration of the algorithm.  $\mathbf{r}$  is a two-dimensional vector describing a point in the object plane.  $\Psi_{g,n}(\mathbf{r}, \mathbf{R})$  is the exit wavefield we calculate when our current estimate of the object function,  $O_{g,n}(\mathbf{r})$ , is illuminated by an illumination function (‘probe’ function),  $P(\mathbf{r}-\mathbf{R})$ , shifted from the origin by a two-dimensional vector quantity,  $\mathbf{R}$ . When this exit wave has been propagated to the far-field, corrected in modulus according to measured data, and propagated back, we find  $\Psi_{c,n}(\mathbf{r})$ ,

where the subscript  $c$  implies this exit wave has been corrected to be consistent with the measured data.  $O_{g,n+1}(\mathbf{r})$  is then made up of two terms: the current running guess of the object function,  $O_{g,n}(\mathbf{r})$ , plus a term constructed from the difference between  $\Psi_{c,n}$  and  $\Psi_{g,n}$ . We put

$$O_{g,n+1} = O_{g,n}(\mathbf{r}) + U(\mathbf{r})(\Psi_{c,n}(\mathbf{r}, \mathbf{R}) - \Psi_{g,n}(\mathbf{r}, \mathbf{R})), \quad (1)$$

where  $U(\mathbf{r})$  is what we call an ‘update function’. This update function can have many forms which we have explored extensively. In this paper, we use a particularly favourable form for thin objects, namely

$$U(\mathbf{r}) = \frac{|P(\mathbf{r}-\mathbf{R})|}{|P_{\max}(\mathbf{r}-\mathbf{R})|} \frac{P^*(\mathbf{r}-\mathbf{R})}{(|P(\mathbf{r}-\mathbf{R})|^2 + \delta)}, \quad (2)$$

where  $P_{\max}$  is the maximum modulus value of  $P$ , and  $\delta$  is a constant determined by the total number of counts in a typical diffraction pattern, and which is used to suppress noise, in a way identical to a Wiener filter in conventional deconvolution methods. Note that this update process is quite unlike any conventional iterative update (for example, Fienup’s HIO algorithm [2]). Its form necessarily derives from the fact that both  $P$  and  $O$  are fully complex functions, and that  $P$  may be soft, bandwidth-limited and possibly of infinite extent, even though it must be ‘substantially’ localised (say in the form of a STEM probe). As described elsewhere [12], the key to the success of the algorithm is to shift the solution of the subsequent guess of the object function by a fractional amount, proportional to the amplitude of the illumination function at any one point over the image plane. Without this modification, the solution is extremely ill-conditioned in the presence of noise and at any region where (in calculating the current new guess of the object) the illumination function is weak. Physically, this is equivalent to giving greater weight to parts of the exit wavefield which have had the biggest influence on the recorded diffraction patterns.

As subsequent data from adjoining areas of the object are fed into the algorithm, a solution quickly appears. Although a new (unknown) part of the object is introduced at each illumination position, the ratio of measured data to unknowns is increased. Of course, once data have been collected, it is both possible and advantageous to re-iterate using data from previous values of  $\mathbf{R}$ . So for example, if we only used three experimental diffraction patterns, labelled 1, 2 and 3, then for  $n = 1, 2, 3, 4, \dots$ , we could use data from positions 1, 2, 3, 1, 2, 3, 1, 2, 3, etc., or indeed in any other order. Each entire pass over all diffraction patterns (in the present case, 100 patterns) we will call ‘one iteration’, although in fact 100 iterations of the update function have occurred in this process.

Two images are obtained: one represents the absorption of the object, shown in Fig. 2a (after 150 iterations over all illumination positions), analogous to a bright field image; the other gives a quantitative phase distribution of the exit

wave (Fig. 2b). The background phase ramp arises from the cover slip not being parallel with the mounting slide. Note that conventional Zernike phase imaging (or conventional bright-field transmission electron imaging), lose low frequencies image components, and so would be unable to detect such large scale phase variation.

We thus reconstruct the total exit wavefield, similar to that encoded in a hologram, but obtained without the use of a reference wave, lens or interferometer of any kind.

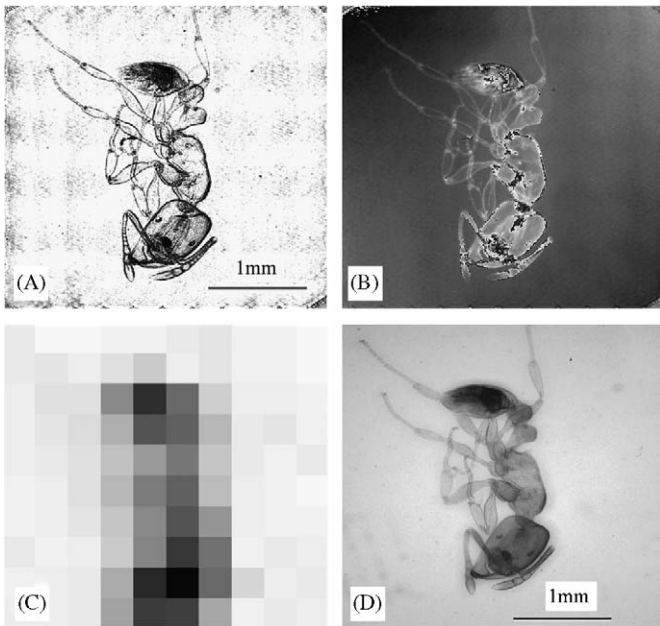


Fig. 2. Images of the object function; illumination conditions are as in Fig. 1. (A) Modulus of the reconstructed image of the object after 150 iterations: dark features correspond to absorption. (B) Phase of the reconstructed object, corresponding to its optical thickness. Sharp changes in intensity correspond to phase wraps of  $2\pi$  in thick areas of the object. The background phase ramp is due to the cover slip not being perfectly parallel to the mounting slide, indicating that our method reconstructs large scale phase changes which are normally invisible in conventional Zernike phase plate imaging. (C) Image obtained by scanning the aperture across the object to the same positions used in the reconstruction: this represents the intrinsic, unprocessed resolution of the optical configuration. (D) Conventional bright-field image obtained on a  $100\times$  microscope.

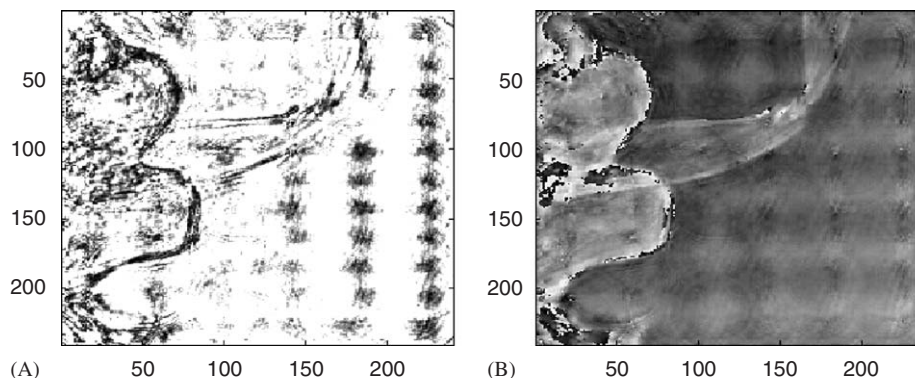


Fig. 3. Modulus (A), and phase (B), obtained with the detector close (15 mm) to the object. The aperture used was  $150\ \mu\text{m}$  in diameter and the nominal resolution of this image is  $3\ \mu\text{m}$ . However, because the detector is no longer formally in the Fraunhofer diffraction plane (by several factors), errors occur. The reconstruction is nevertheless reasonable.

This is a crucial advantage of the technique: it is not dependent on wavelength-scale stability or coherence: a particularly severe limitation in electron imaging. Fig. 2c shows the image we obtain by scanning our object across the illumination function and simply detecting the transmitted intensity. For comparison, Fig. 2d shows the conventional bright-field lens image of the same object obtained on a  $100\times$  objective optical microscope.

The resolution of our reconstruction is determined by the angular size of the diffraction pattern we process, which is limited geometrically by the size of our CCD camera and the camera length. In the image presented in Figs. 2a and b, we process only a semi-angle of  $37\ \text{mrad}$ , giving an intrinsic resolution of  $17\ \mu\text{m}$ . The reconstruction has been performed with an image pixel size of  $13\ \mu\text{m}$ . The important difference to note is between Fig. 2c and Figs. 2a and 2b: the effective gain in resolution over the intrinsic resolution of our only imaging component—a simple aperture—is a factor of 47. In the case of scanning transmission electron microscopy (STEM), it is routinely possible to obtain a  $0.2\ \text{nm}$  probe (illumination) function. A similar gain in resolution would then achieve ultimate wavelength-limited imaging (about  $\frac{1}{100}$  of an atomic diameter): only the zero-point energy of the atomic vibrations would define useable resolution. Even in conventional light optical imaging, no longer requiring a lens that is mounted close to the sample would have important benefits. For example, remote imaging will in principle allow uncompromised resolution to be obtained for objects held within pressurised or environmental enclosures. Furthermore, since we have recovered the entire wavefunction, all depth information is also encoded in our data, leading to the possibility of 3D imaging without lenses.

In Figs. 3a and b, we present the amplitude and phase of a reconstruction using no lenses at all. In order to make our simple detector possess a large angle effective numerical aperture, we have moved it to a position just  $15\ \text{mm}$  downstream of the object. The aperture we employ in this experiment is  $150\ \mu\text{m}$  in diameter. The nominal resolution of the reconstruction (part of the ant shown in Fig. 2) is  $3\ \mu\text{m}$ : this increase is due to the larger scattering angle we

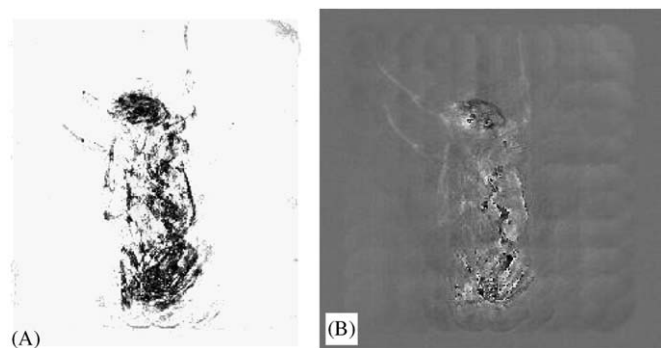


Fig. 4. Modulus (A), and phase (B), obtained from just one iteration of the algorithm. Most pertinent features of the object are visible, showing that reasonable quality imaging can be obtained for large fields of view in real time.

can process in this configuration. However, even with such a small aperture, the Fraunhofer condition is far from satisfied. In the present case,  $D^2/\lambda$ , where  $D$  is the diameter of the aperture, has a value of 30 mm. It is usual to require  $D^2/\lambda$  to be several factors larger than this order for the Fraunhofer condition to be fully satisfied. In other words, with our detector at 15 mm, we are really in the Fresnel zone, yet blind application of the algorithm, which in this case is assuming the propagator is a Fourier transform, still produces an interpretable image. The limited degradation in the image only occurs when the technique is used with relatively long wavelength radiation (i.e. light optical).

By recording more than one diffraction pattern from adjacent regions of the object, our data have redundancy which the algorithm uses to good effect. Ambiguous solutions which can sometimes arise in conventional iterative methods are suppressed; solving for complex (real and imaginary) transmission objects is fast and routine. The redundancy leads to remarkable insensitivity to noise evidenced by the relatively low performance CCD camera we have employed in this experiment. Moving the illumination yields an alternative solution to the phase problem called ptychography [14–20]. This is why we refer to our method as PIE: it amounts to a ‘ptychographic iterative engine.’ As a result of this much richer information, a recognisable image emerges from the algorithm after just one Fourier iteration per illumination position (see Figs. 4a and b): most iterative methods require thousands or tens of thousands of iterations to achieve a good result. As a consequence, using our new method, large areas of specimen can be surveyed in real time, as fast as in a conventional microscope.

#### 4. Conclusions

For the first time, we have demonstrated experimentally, using light optics, a new type of lensless imaging which will ultimately provide wavelength-limited resolution for objects of unlimited lateral size or shape. The new imaging method can be implemented for any type of radiation and, in the case of X-ray or electron imaging, the technique we have demonstrated here should deliver important gains in resolution over present lens configurations, again for objects of any size, and in real time. This would in principle provide spectacular sub-atomic wavelength-limited resolution, even when using relatively poor lenses (to produce a confined illumination), or even no lenses at all.

#### Acknowledgements

A.C.H. is supported by an EPSRC doctoral training account. We thank C. Rodenburg for acquiring the conventional optical image.

#### References

- [1] E. Abbe, Arch. Mikrosk. Anat. 9 (1873) 413.
- [2] J.R. Fienup, Appl. Opt. 21 (1982) 2758.
- [3] J.C.H. Spence, U. Weierstall, M. Howells, Philos. Trans. R. Soc. London A 360 (2002) 875.
- [4] J. Miao, P. Charalambous, J. Kirz, D. Sayre, Nature 400 (1999) 342.
- [5] J.M. Zuo, I. Vartanyants, M. Gao, R. Zhang, L.A. Nagahara, Science 300 (2003) 1419.
- [6] J. Wu, U. Weierstall, J.C.H. Spence, Nature Mat. 12 (2005) 912.
- [7] R.W. Gercherg, O. Saxton, Optik 35 (1972) 237.
- [8] D.L. Misell, J. Phys. D: Appl. Phys. 6 (1973) 2200.
- [9] L.J. Allen, M.P. Oxley, Opt. Commun. 199 (2001) 65.
- [10] W. Hoppe, Acta Cryst. A 25 (1969) 508.
- [11] H.M.L. Faulkner, J.M. Rodenburg, Phys. Rev. Lett. 93 (2004) 023903/1.
- [12] J.M. Rodenburg, H.M.L. Faulkner, Appl. Phys. Lett. 85 (2005) 4795.
- [13] H.M.L. Faulkner, J.M. Rodenburg, Ultramicroscopy 103 (2004) 153.
- [14] J.M. Rodenburg, H.M.L. Faulkner, UK patent application PCT/GB2005/001464 ‘High resolution imaging’, 2004.
- [15] R. Hegerl, W.P. Hoppe, Proceedings of the Fifth European Congress on Electron Microscopy, Institute of Physics, London, 1972, p. 628.
- [16] R. Hegerl, W. Hoppe, Ber. Bunsenges. Phys. Chem. 74 (1970) 1148.
- [17] J.M. Rodenburg, R.H.T. Bates, Philos. Trans. R. Soc. A 339 (1992) 521.
- [18] P.D. Nellist, B.C. McCallum, J.M. Rodenburg, Nature 374 (1995) 630.
- [19] P.D. Nellist, J.M. Rodenburg, Acta Crystallogr. A 54 (1998) 49.
- [20] T. Plamann, J.M. Rodenburg, Acta Crystallogr. A 54 (1998) 61.